Project no. TIP5-CT-2006-031415

INNOTRACK

Integrated Project (IP)

Thematic Priority 6: Sustainable Development, Global Change and Ecosystems

D3.1.4 Summary of results from simulations and optimisation of switches

Due date of deliverable: 2008/12/31

Actual submission date: 2009/02/13

Start date of project: 1 September 2006 Duration: 36 months

Organisation name of lead contractor for this deliverable: Chalmers

Revision Final

Project co-funded by the European Commission within the Sixth Framework Programme (2002-2006)		
Dissemination Level		
PU	Public	X
PP	Restricted to other programme participants (including the Commission Services)	
RE	Restricted to a group specified by the consortium (including the Commission Services)	
CO	Confidential, only for members of the consortium (including the Commission Services)	

Table of Contents

Table of figures

Glossary

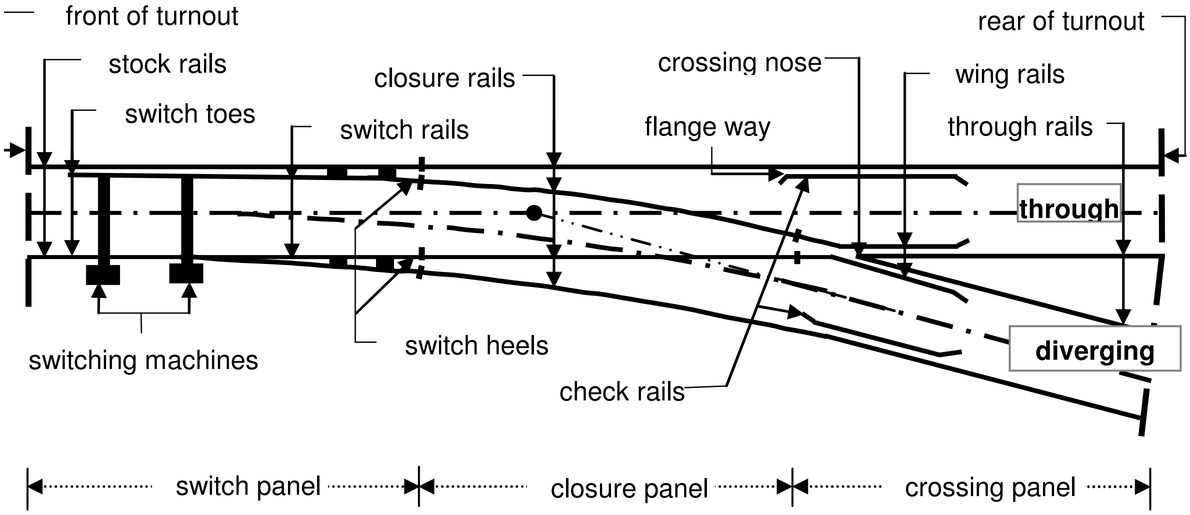

Components of a turnout with through and diverging routes. From [1]

1. Executive Summary

The work in INNOTRACK SP3.1 (tasks 3.1.5 Materials and 3.1.6 Optimisation) aims at the development of innovative S&C (Switches & Crossings) designs that allow for increased axle loads and speeds and lead to decreased need for maintenance.

INNOTRACK deliverable 3.1.4 provides an extended summary of the work performed up to December 2008. It contains three parts:

1. The optimisation of S&C is mainly based on numerical simulations. Since simulation work is shared between different partners (Chalmers, DB, MMU and VCSA), it was necessary to *develop a common simulation platform*. To ensure that the results of the simulations are comparable and represent reality correctly, it was decided to perform a *validation* of the different software used on the basis of results from *field measurements* in Härad (Sweden). The first part of the report describes the field test in Härad and presents a comparison of measured and calculated wheel–rail contact forces.
2. *Optimisation of dynamic track gauge in the switch panel*

   Railway vehicles often experience significant lateral displacements, sometimes leading to wheel flange contact, when running in the through route of the switch panel. This often creates increased wheel and rail wear and sometimes rolling contact fatigue problems on the rails, requiring increased supervision and maintenance and reducing the life of the components.

   The geometry of the gauge variation in the switch panel is in the study represented in a parametric way. Based on a parametric study, two possible optimal solutions were found and validated by evaluating a wider set of simulation cases. The main benefits obtained by the new designs proposed are (i) a significant *reduction of wear*, represented by $T\gamma$, in all locations analysed along the switch, and (ii) a significant *reduction of traction coefficient*, and therefore improved behaviour in terms of *rolling contact fatigue.*
3. *Optimisation of geometry and support stiffness in the crossing panel*

   Severe impact loads may be generated when the wheels are transferred between wing rail and crossing nose in the crossing panel. The objective of this study was to optimise the crossing geometry and the support stiffness of the superstructure in order to reduce the contact stresses induced by the wheels. Different modifications of crossing nose and wing rail profiles are proposed and compared based on numerical simulations.

   The comparison of standard support stiffness with reduced support stiffness (by means of elastic rail pads) shows that the *impact loads can be reduced* considerably especially for crossing negotiation at high speed. Investigations of different crossing geometries show that it is difficult to find a solution which leads to a force reduction for all wheel profiles occurring in service. Nevertheless, the MaKüDe crossing design showed the best performance especially for mean worn wheel profiles for both running directions (facing and trailing moves). In connection with reduced support stiffness (e.g. elastic rail pads), this crossing design will lead to a significant reduction of the impact loads and consequently a high *potential for LCC reduction*.

Full details on the work summarised here are given in separate reports appended to this deliverable:

- E Kassa and J C O Nielsen, Dynamic interaction between train and railway turnout – full-scale field test and validation of simulation models. *Vehicle System Dynamics* Vol 46, Issue S1 & 2, 2008, 521-534 (Appendix A in D3.1.4)
- D Nicklisch, Validation of a SIMPACK model for simulation of turnout passing, INNOTRACK Technical report, April 2008, 13 pp (Appendix B in D3.1.4)
- J Perez, Optimisation of the dynamic gauge for railway switches, INNOTRACK Technical report, December 2008, 25 pp (Appendix C in D3.1.4)
- D Nicklisch, SIMPACK-simulations of passing switches and crossings, INNOTRACK Technical report, December 2008, 11 pp and two appendices (Appendix D in D3.1.4)

2. Introduction

The work in INNOTRACK SP3.1 (tasks 3.1.5 Materials and 3.1.6 Optimisation) aims at an optimisation of S&C (Switch & Crossing) geometry and the development of innovative switch designs in order to allow for increased axle loads and speeds and decreased maintenance.

To meet these aims, simulation tools are used to calculate wheel-rail contact forces at key components in a switch. These tools have been validated with respect to results from a field test, providing a common platform for the optimisation work. The design variables in the optimisation include: rail inclination, track gauge, rail profiles, support stiffness, crossing geometry and material. Attention is given to freight vehicles with high axle loads and the type of traffic at selected demonstrator sites.

The present report provides an extended summary of the work performed up to December 2008. The current deliverable (Deliverable 3.1.4) contains three parts:

1. A comparison of measured and calculated wheel–rail contact forces. The forces calculated by use of SIMPACK and GENSYS are compared with results from a field test in Härad, Sweden (contributions by Chalmers, DB, MMU and VCSA)
2. Optimisation of dynamic track gauge in the switch panel (MMU)
3. Optimisation of crossing geometry (DB and VCSA)

The full details of the Härad field test, the validation of simulation software and the optimisations of crossing geometry and dynamic track gauge are provided in the separate reports:

- E Kassa and J C O Nielsen, Dynamic interaction between train and railway turnout – full-scale field test and validation of simulation models. *Vehicle System Dynamics* Vol 46, Issue S1 & 2, 2008, 521-534 (Appendix A in D3.1.4)
- D Nicklisch, Validation of a SIMPACK model for simulation of turnout passing, INNOTRACK Technical report, April 2008, 13 pp (Appendix B in D3.1.4)
- J Perez, Optimisation of the dynamic gauge for railway switches, INNOTRACK Technical report, December 2008, 25 pp (Appendix C in D3.1.4)
- D Nicklisch, SIMPACK-simulations of passing switches and crossings, INNOTRACK Technical report, December 2008, 11 pp and two appendices (Appendix D in D3.1.4)

A final deliverable covering the remaining work in tasks 3.1.5 and 3.1.6 is due on 2009-07-31. That report will contain results from further work on the optimisation of switch geometry and the influence of material selection on geometry degradation in the switch due to plastic deformation and wear.

3. The Härad field test – Chalmers

In May 2006, a field measurement campaign was carried out in a turnout (switch & crossing) in Härad in Sweden [1]. The turnout design and the measured results from Härad are being used as reference in much of the work performed in INNOTRACK SP3.1. For example, wheel–rail contact forces measured in the turnout have been used to validate the computer models used in the project.

Output data from the measurements included lateral (*Y*) and vertical (*Q*) wheel–rail contact forces from an instrumented wheelset that was positioned as the leading wheelset (when travelling in the facing move) in the leading Y25 bogie of a freight vehicle. During the measurements, the freight vehicle passed the turnout in both the main and diverging routes at different speeds. The turnout was a design (UIC60-760-1:15) diverging to the right with curve radius 760 m, crossing angle 1:15 and 60E1 rails, see Figure 1.

Wheel profiles were measured using MiniProf equipment. Rail profiles were also measured using MiniProf at some 80 positions on the left and right rails in the through and diverging routes. Track gauge was measured at the same positions. The rail profiles and track gauge were measured at every 10 cm in the crossing panel and at every 30 cm in the switch panel. Track irregularities were not measured.

Figure 1 - UIC60-760-1:15 turnout in Härad. From [1]

The following data were supplied to all simulation partners, see Ref. [2]:

- Lateral (*Y*) and vertical (*Q*) wheel–rail contact forces measured with sampling frequency 9.6 kHz. Contact forces were supplied for two load cases: facing move of diverging route at 60 km/h and facing move of through route at 100 km/h
- Wheel profiles
- Rail profiles and deviations from nominal track gauge
- Track receptance data from impact tests
- Y25 bogie data

Calculated wheel–rail contact forces are compared with measured forces in Section 4.

The field test and the evaluated results are described in detail in Ref. [1]. One example of results from [1] is shown in Figure 2. Based on the results from the field measurements, the influences of train speed, route and running direction on the maximum vertical contact force (impact load) Q_{max} at the crossing are displayed. For all train routes, an increase in Q_{max} with increasing train speed is observed. However, the increase in impact load is considerably higher for the diverging route as compared to the through route. In the through route, the contact force increases by a moderate 15 % when train speed increases from 10 km/h to 80 km/h. The corresponding increase in the diverging route is about 40 %. The influence of running direction (from wing rail to crossing nose in the facing move or vice versa in the trailing move) on Q_{max} is relatively small for both the through and diverging routes.

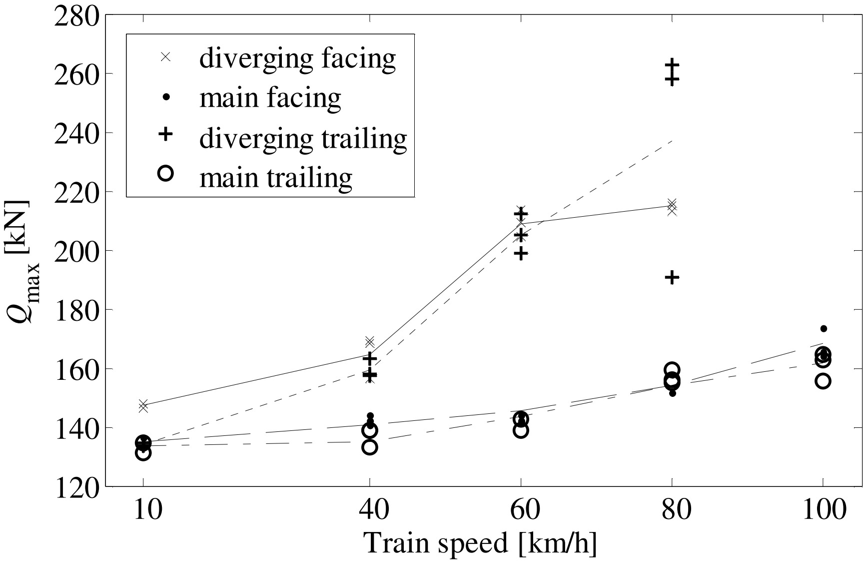

Figure 2 - Measured maximum vertical contact force (impact load) Qmax when the train is moving in the through or diverging route and in the facing or trailing move. The lines are least square fits to the measured values. From [1]

4. Common simulation platform – validation of models

INNOTRACK subproject 3.1 “Switches & Crossings” contains several tasks which need to be treated by means of numerical simulation. Because this simulation work is shared between different partners (Chalmers, DB, MMU and VCSA) using different computer programs, it was necessary to develop a common simulation platform. This does not mean that all partners must use the same software package and the same simulation model, but it had to be ensured that the results of the simulations are comparable and represent reality correctly.

This is why it was decided to perform a validation test on the basis of the field measurements in Härad. To make this possible, Chalmers provided measurement data from a freight vehicle passing through the turnout, see Refs. [1,2]. Based on these data, all partners involved in simulation work performed calculations to compare their predicted results with the measurements.

4.1 SIMPACK – modelling by DB

Results from the DB simulations of dynamic train–track interaction in Härad using the software SIMPACK are described in detail in Ref. [3].

The track model is a finite element model (FEM) consisting of elastic rails and elastically supported elastic (concrete) sleepers which are arranged according to the layout of the turnout. The changing dynamic properties of the track within the turnout are represented by position dependent parameters such as rail cross-section and sleeper mass. The values were chosen according to a common ballasted track turnout at DB.

Comparisons of time histories of measured Y and Q forces in the diverging route with the corresponding simulated forces are presented in Figs. 3 and 4. A low-pass filter with cut-off frequency 100 Hz has been applied. This eliminates the higher frequency noise from the measurements to allow for a comparison with the relatively low-frequency simulation results. The influence of the curve entry (the curve starts at s = 30 m) and the contact with the check rail in the crossing area can clearly be seen. In general there is good agreement between measurement and simulation, but in the crossing area where check rail contact occurs, the calculated maximum Y forces are significantly lower than the measurement results. This could be caused by the lack of information about profile and position of the check rail. The dynamics in the crossing area (transition from wing rail to crossing nose) is well represented in the simulation. Further comparisons of measured and calculated contact forces are presented in Ref. [3].

The purpose of this investigation was to demonstrate that simulation of vehicles passing a turnout is feasible with good results. This could be shown in principle even though there are some differences between measured and calculated wheel-rail contact forces. To achieve a better agreement between measurement and simulation, additional information is necessary such as measured check rail clearance and track irregularities (longitudinal level, alignment).

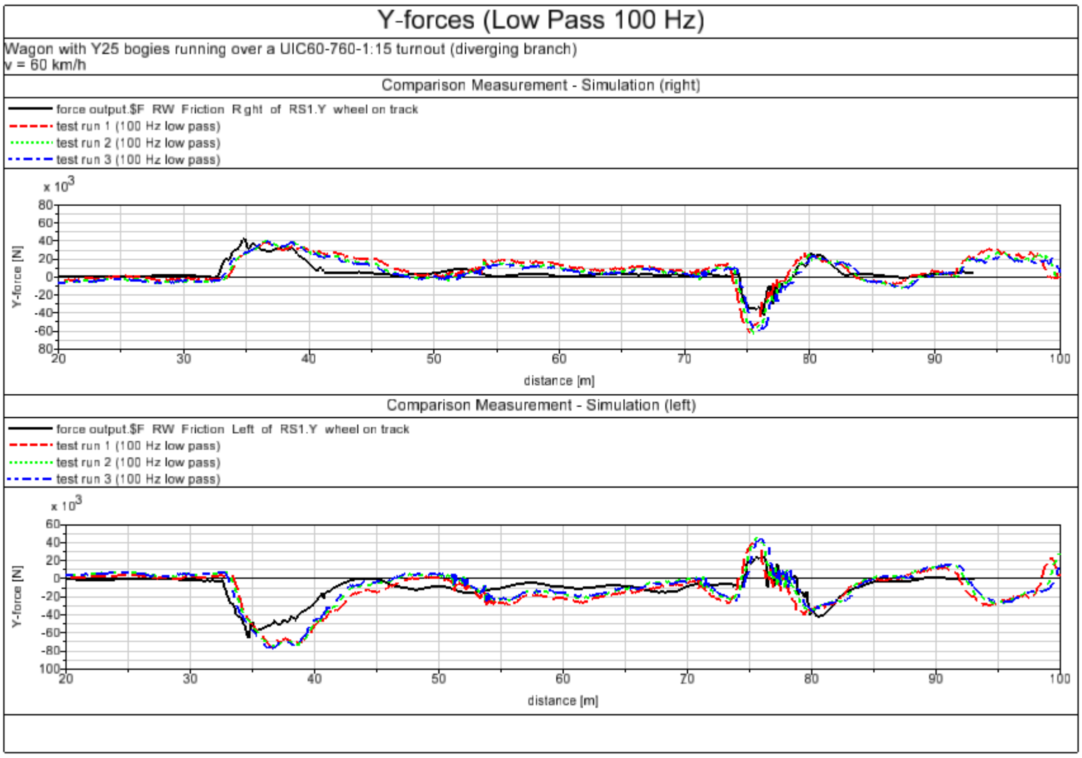

Figure 3 - Comparison of measured and calculated lateral wheel–rail contact forces. Load case: facing move of diverging route in Härad at 60 km/h

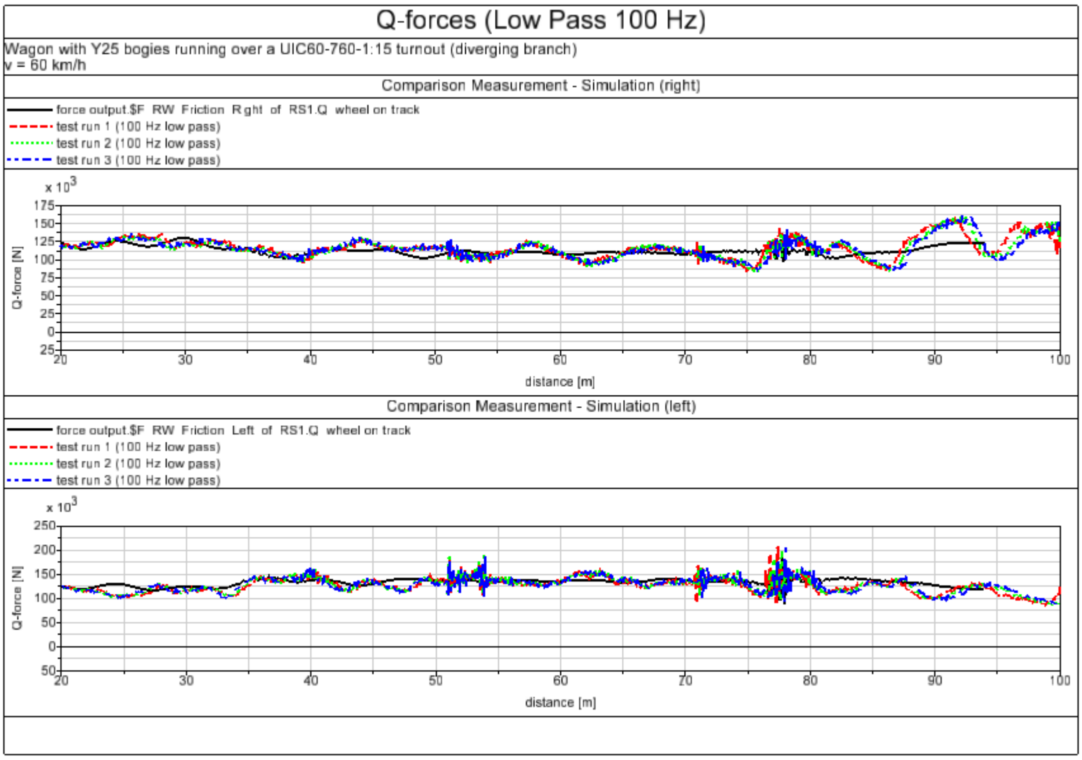

Figure 4 - Comparison of measured and calculated vertical wheel–rail contact forces. Load case: facing move of diverging route in Härad at 60 km/h

4.2 SIMPACK – modelling by MMU

The Rail Technology Unit at MMU also uses SIMPACK as one of the modelling tools for their work. The major difference compared to the modelling by DB is the type of track model adopted.

4.2.1 Features of the implementation of the Härad turnout

- Rail profiles: Miniprof measurements of the rail profiles were available as outlined in section 3. Lateral and vertical alignment prior to their implementation as a "Variable S-profile" model in SIMPACK. This is pre-processed in SIMPACK. The resulting S-variable profile is thoroughly reviewed, and some of the original profiles are modified (mainly extending or shortening one of the sides) so that the resulting interpolated profiles are realistic.
- Track geometry: The track geometry is modelled simply as a constant radius curve with a very short curve transition. The only track irregularity modelled is track gauge, for which data was available. Lateral and vertical irregularities were not available.
- Track form flexibility: In this work the standard model of flexible track from SIMPACK was used, seeFigure 5. It is a lumped mass-system consisting of just one mass per wheelset that "follows" the wheel/rail contact and with stiffness acting in the lateral, vertical and roll degrees of freedom. This simple model was tuned to fit, in the best possible way, to the measured receptances. The vertical stiffness was fitted to the receptance measured at the crossing nose, while the lateral stiffness was fitted to the receptance measured at the switch blade location.

The model i s clearly too simplified to adequately represent the measured receptances but, as will be shown in the next sub-section, it gave acceptable results this time. This standard model can be extended manually to include multiple masses and stiffnesses, which has been shown by some researchers to work well up to 150 Hz – 200 Hz [4].

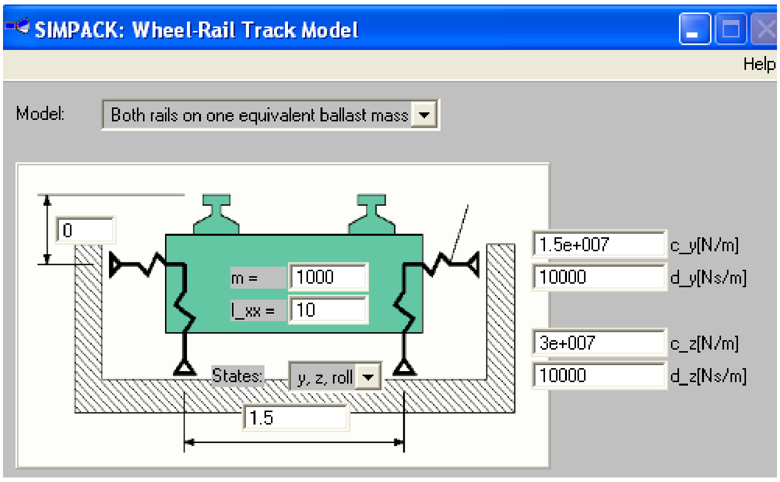

Figure 5 - Parameters of the flexible track model

- W/R Contact parameters in SIMPACK: The wheel/rail contact forces are modelled using the simplified Kalker method (Fastsim). The forces are evaluated online during the calculation. The value used for the friction coefficient was 0.35. The elasticity at the contact is considered through a stiffness of $5{\cdot}10^8$ N/m at the tread and flange and $5{\cdot}10^7$ N/m at the back of the wheel.

4.2.2 Construction of the turnout model

The following steps have been followed to build the turnout model from the existing data:

- Selection of rail profiles and positions to be used and convertion to SIMPACK format: All the profiles provided were used in the simulation. Two new profiles were added:
    - At the position 11.260 m, a new profile was superimposed. The new profile is exactly the same geometry as the original, but a part of it has been removed in order to get an adequate interpolation with both the previous and the following rail profiles.
    - At the position 46.800 m, a new rail profile was added to the left rail. This point is considered to be where the gauge widening near the crossing nose is a maximum, and the new profile is meant to represent this. The new profile added is exactly the same geometry as the original, but it has been moved laterally according to the gauge widening expected in this position.
- Changes to rail profiles: the rail profile section files have been opened individually and modified if required. The modifications consist of either extending or trimming the profile. The criteria for the modifications are that any interpolation between each profile and the next should be carried out in the same zone of the profile (i.e. the gauge corner of one profile must be interpolated with the gauge corner of the next). This process was carried out iteratively by looking for unusual shapes in the interpolations.
- Generation of the SIMPACK S-Variable rail models: the profiles were used to generate rails through the switch using the SIMPACK ‘S-Variable’ facility.

4.2.3 Vehicle model

A Y25 bogie based vehicle model is used in the simulations. A generic SIMPACK model of this vehicle has been provided by Deutsche Bahn. This model has been modified by MMU to match the parameters of the real vehicle provided by Chalmers.

4.2.4 Results and validation

Lateral forces

Figure 6 and Figure 7 show a comparison of the lateral wheel–rail contact forces measured by the instrumented vehicle and those obtained by simulation. The magnitude and location of the main features in the force history at the switch rail are well predicted by the model at both the switch blade and the crossing. There are some relatively small differences, which can be mainly due to the fact that no vertical or lateral track irregularities were included in the simulation.

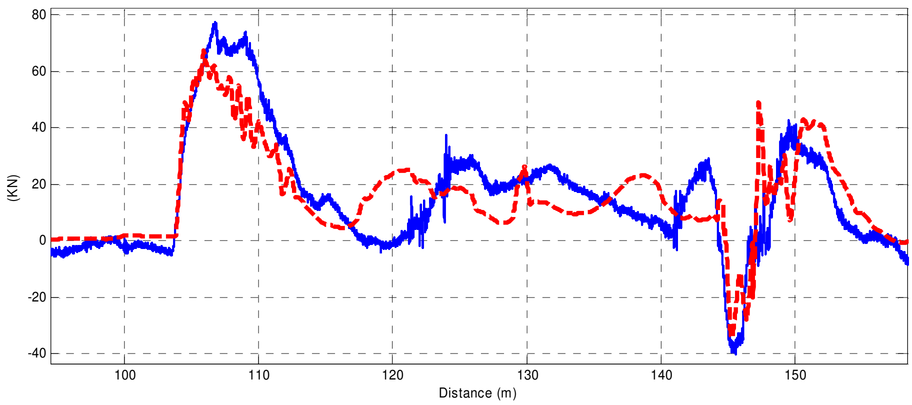

Figure 6 - Lateral forces left rail (switch rail) - Measured (solid) vs. simulated (dashed). Load case: facing move of diverging route in Härad at 60 km/h. Locations of switch toe (x = 100.81 m), switch heel (x = 122.6 m), crossing nose (x = 146.9 m), and check rail span (143.1 m < x < 150.9 m), where x is the distance from front of turnout.

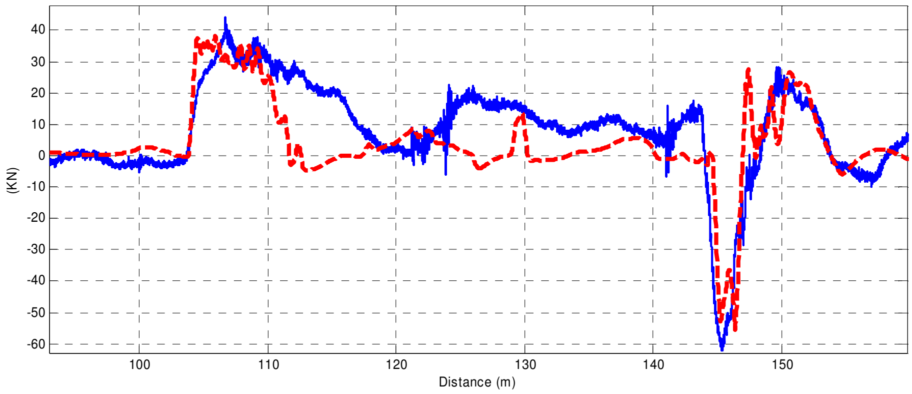

Figure 7 - Lateral forces right rail (stock rail) - Measured (solid) vs. simulated (dashed). Load case: facing move of diverging route in Härad at 60 km/h. Locations of switch components: see legend of Figure 6.

Vertical forces

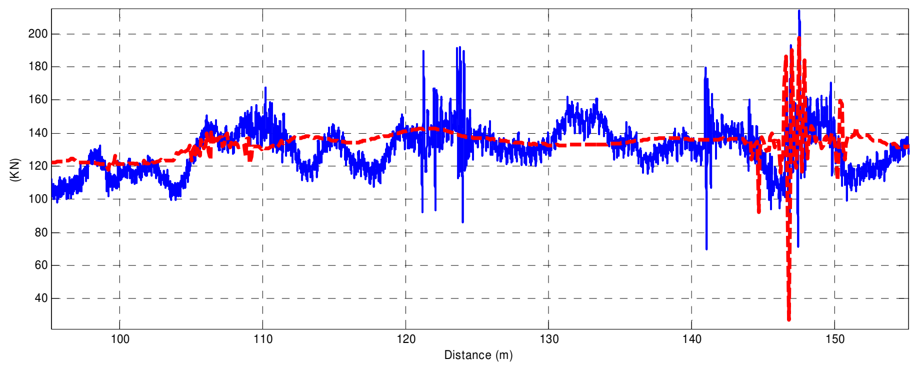

Figure 8 - Vertical forces left rail (switch rail) - Measured (solid) vs. simulated (dashed). Load case: facing move of diverging route in Härad at 60 km/h. Locations of switch components: see legend of Figure 6.

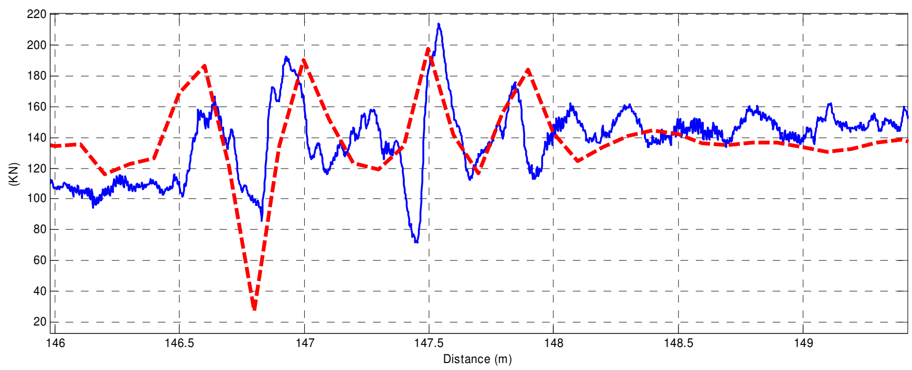

Figure 9 - Vertical forces around the crossing - Measured (solid) vs. simulated (dashed). Load case: facing move of diverging route in Härad at 60 km/h. Locations of switch components: see legend of Figure 6.

A comparison of measured and calculated vertical contact forces is shown in Figure 8. The simulation predicts reasonably well the general vertical loads, but it does not predict at all some relatively low frequency oscillations. This is most probably due to the fact that the vertical alignment of the track was not measured and therefore it could not be included in the model. One of the main interests in the plot of the vertical forces is the representation of the forces at the impact between the wheel and the nose. The performance of the model at this location is shown in Figure 9.

The location and magnitudes of the main peaks seem to be reasonably well represented. However there is clearly a lack of higher frequency information in the simulation, due to the relatively simple elastic track model. This match could be improved if the track model was extended with more masses and stiffness elements.

4.2.5 Comments and conclusions

The comparison between the simulation results and the experimental results is considered acceptable. The simulation retains the main features of the measured forces, and shows similar magnitudes. There are a number of differences in the magnitudes, but it must be taken into account that there are several uncertainties present, such as:

- The friction based vehicle model has not been validated against the real one. There are parameters important to its behaviour, such as the friction coefficients in the suspension, which can differ significantly from the actual vehicle.
- Vertical and lateral track irregularities are not known.
- Wheel/rail coefficient of friction is not known.
- Measurement uncertainties (calibration, etc) can also have some (probably minor) effect on the measured results

Taking these considerations into account, the performance of the simulation model is considered satisfactory for the work being carried out in INNOTRACK.

Some final comments that reflect some of the limitations of the methodology and the tools used:

- The interpolation of rail profiles can cause problems when there are very abrupt changes in the shape between contiguous rail profiles. The solution most typically used is to overlap two equal profiles, extending one of them so that it fits adequately with the subsequent one. However, this often leads to spikes in the simulation results.
- The track model used here does not provide adequate high-frequency behaviour. A simple extension of the lumped mass model can be implemented to increase the frequency range of the model up to around 200 Hz [4].

4.3 GENSYS – modelling by Chalmers

In the simulations performed by Chalmers, the multi-body system (MBS) software GENSYS was used [5]. The vehicle model [6] is a freight vehicle including two Y25 bogies. Coulomb friction is used in the bogie model for the couplings of the two side beams with the transverse centre beam, and for the coupling of the car body with the transverse centre beam.

To model track dynamics in the low-frequency range 0 – 20 Hz, one co-following mass-spring-damper system with few degrees-of-freedom is coupled to each wheelset (moving track model). Each track model contains two rails with neglected inertia that are attached to a track mass by spring-damper elements in lateral and vertical directions. The spring-damper elements account for the flexibility of rail, rail pad and rail fastener. The remaining track flexibility is represented by spring-damper elements that connect the track mass to a rigid ground. The wheel–rail contact model is based on Hertz linearised contact and FASTSIM, and accounts for two-point contact situations. Variations in rail profile and track gauge along the turnout are accounted for. The wheel–rail contact geometry is treated by pre-calculated look-up tables. Using an interpolation procedure, the contact geometry functions are used in the subsequent time integration.

Results from simulations with the model of train–turnout interaction were compared with measurements from Härad. The measured contact forces were low-pass filtered using the cut-off frequency 1 kHz.

Figures 10 and 11 show the measured and simulated contact forces on the left and right wheels when diverging route and train speed (60 km/h) were considered. The transient behaviour of the simulated contact forces is similar to that measured. The profile variation of the left rail generates high-frequency components of the measured force, but this is not captured by the GENSYS model. For both wheels there is a sudden change in both the measured and simulated lateral wheel–rail contact force at about four metres after the front of the turnout. This is because flange contact with the switch rail starts at this position. The increase in measured and simulated lateral contact forces appear in the same region. However, in the switch panel at about 10 m, the measured lateral contact force on the left wheel is somewhat higher than the simulated force, see Figure 10.

In the crossing panel at about 44 m from the front of the turnout, there is a sudden reversal in direction of the lateral contact force on both the left and right wheels. Again, the simulated and measured forces have the same pattern. The measured vertical force on the left wheel contains significant transients at several positions along the turnout, but the general trend is similar to the simulated result, see Fig. 10. On the right wheel, see Fig. 11, the results are in good agreement except at the switch heel and in the crossing panel. The large high-frequency contributions to all measured contact forces around the switch heel at about 20 – 25 m are probably due to the change in the rail height (web height) followed by an insulating joint. This influences the vertical bending stiffness of the track. The corresponding results for the load case main route and 100 km/h are shown in Figs. 12 and 13.

As suggested above, the agreement between measured and simulated contact forces could be further improved if track irregularities in the turnout were known and accounted for in the model. The models and further comparisons with results from the field test in Härad are described in more detail in Ref. [1].

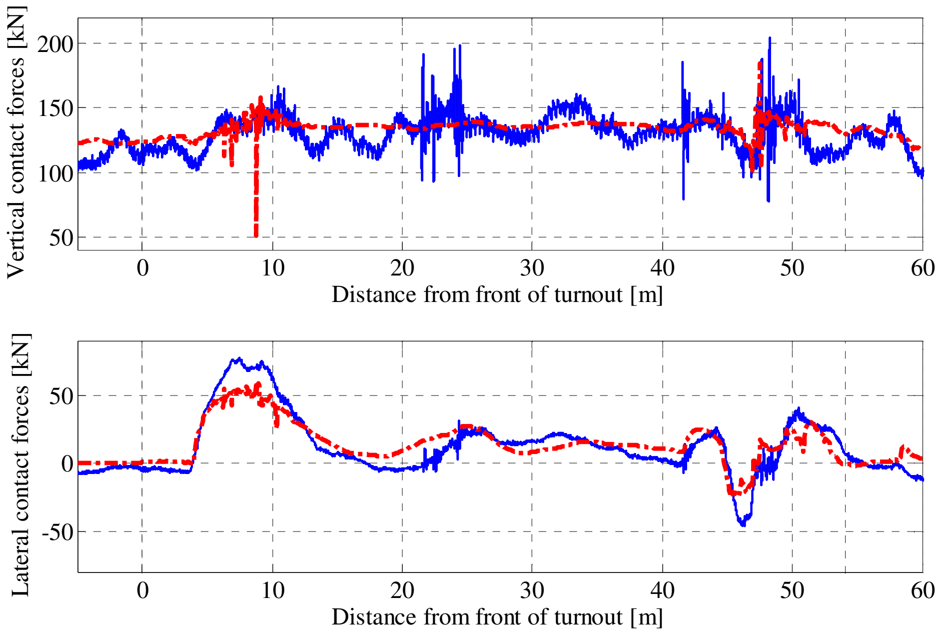

Figure 10 - Vertical and lateral wheel–rail contact forces on the left (outer) wheel of the leading wheelset in the leading bogie. Facing move in the diverging route. Train speed 60 km/h. Measured (solid) vs. simulated (dashed). Locations of switch toe (x = 0.81 m), switch heel (x = 22.6 m), crossing nose (x = 46.9 m), and check rail span (43.1 m < x < 50.9 m), where x is the distance from front of turnout

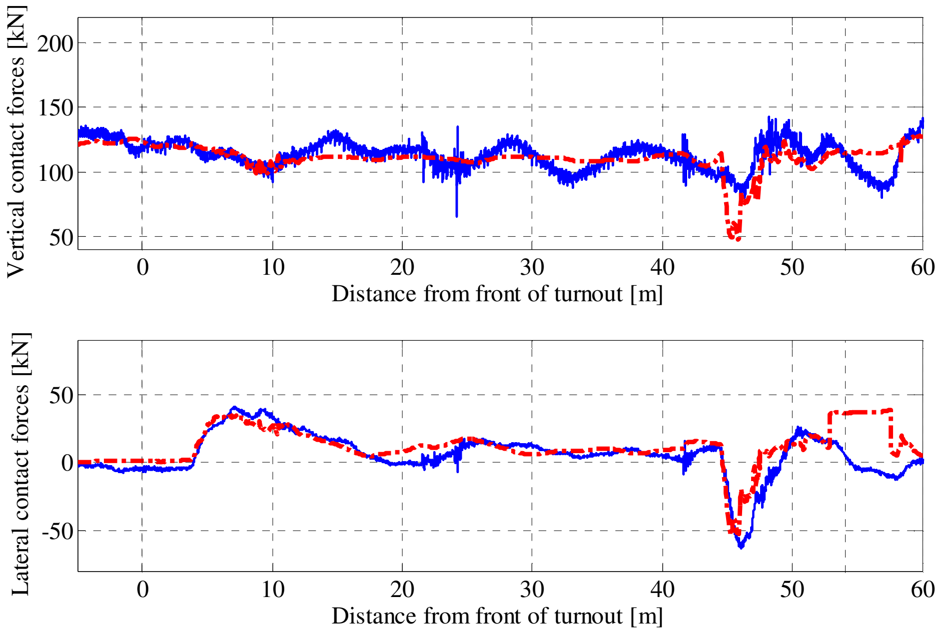

Figure 11 - Vertical and lateral wheel–rail contact forces on the right (inner) wheel of the leading wheelset in the leading bogie. Facing move in the diverging route. Train speed 60 km/h. Measured (solid) vs. simulated (dashed). Locations of switch components: see legend of Figure 10

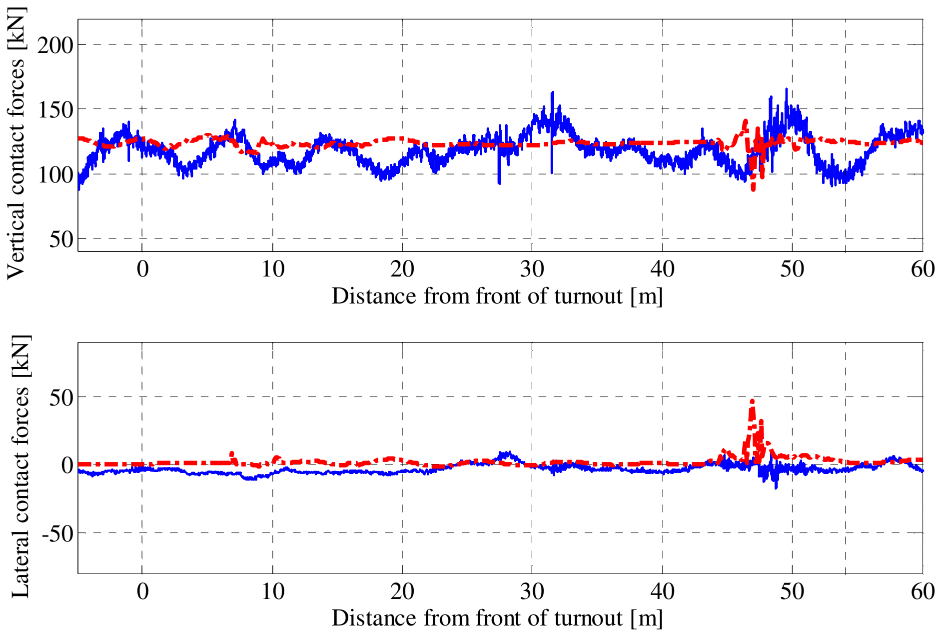

Figure 12 - Vertical and lateral wheel–rail contact forces on the left wheel of the leading wheelset in the leading bogie. Facing move in the through route. Train speed 100 km/h. Measured (solid) vs. simulated (dashed). Locations of switch components: see legend of Figure 10

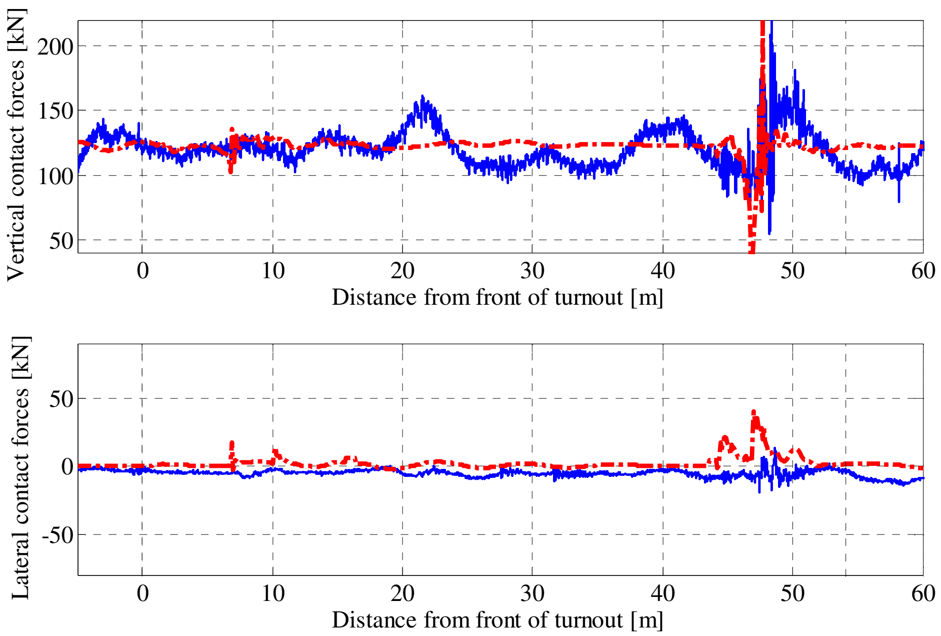

Figure 13 - Vertical and lateral wheel–rail contact forces on the right wheel of the leading wheelset in the leading bogie. Facing move in the through route. Train speed 100 km/h. Measured (solid) vs. simulated (dashed). Locations of switch components: see legend of Figure 10

4.4 BCCM – modelling by VCSA

BCCM (Bouncing Contact Conicity Modelisation) is an in-house computer program developed by VCSA to determine the path of the wheel transfer through the switch. For different prescribed lateral wheelset displacements (sway), the contact point location on the rail and the vertical displacement (bounce) of the wheel are determined based on a pure kinematic calculation, see Figure 14. Both wheelset and track are assumed to be rigid. Only the main route (straight track) is considered.

Lateral wheelset displacements and contact point locations on the rail have been calculated by DB, MMU and Chalmers using SIMPACK and GENSYS for the Härad load case: main route 100 km/h. Based on these lateral wheelset displacements, BCCM has been used to determine the corresponding contact point locations. As input to the calculations, all rail profiles in the switch panel measured in Härad were aligned vertically with respect to the top of the rail and laterally with respect to the gauge point (on the gauge face 14 mm below the top of the rail), see Fig. 15. Contact point displacements are calculated with respect to the gauge point.

To compare BCCM with the kinematic output from SIMPACK and GENSYS, the evaluated contact point locations have been compared in the switch and crossing panels, see Figure 16 to Figure 21. Note that contact point location [mm] is given on the left vertical axis whereas the lateral wheelset displacement (sway) [mm] is given on the right vertical axis.

BCCM is restricted to consideration of situations with one contact point for the corresponding lateral wheelset position. The main differences between the results from BCCM and the MBS programs (SIMPACK/GENSYS) are explained by that there are several situations with two contact points. In these cases, the BCCM contact point is compared to the closest of the contact points from the MBS calculation.

In GENSYS, track gauge irregularities were considered by positioning the origin of the rail based on the measured track gauge widening or track gauge narrowing. In addition, the measured rail profiles contain surface irregularities. In GENSYS, a wheel load of 100 kN was used to determine the contact point as the point with the maximum local deformation within the contact patch, whereas BCCM is a purely kinematic calculation which may locate the closest point between the wheel and rail.

The difference between the MBS models and BCCM may partly also be explained by that the rails in the MBS models are elastically constrained (allowed to deflect) whereas in the BCCM model they are rigid, and that there are occasions with two-point contact situations when there is a transfer between contact points which may be differently influenced by this.

BCCM and SIMPACK interpolate rail geometry between two adjacent cross-sections based on the given geometry of the two sections, while GENSYS determines rail geometry by an interpolation in pre-calculated tables.

BOUNCING :
Difference between the height of the wheel (at the running thread) and the running surface

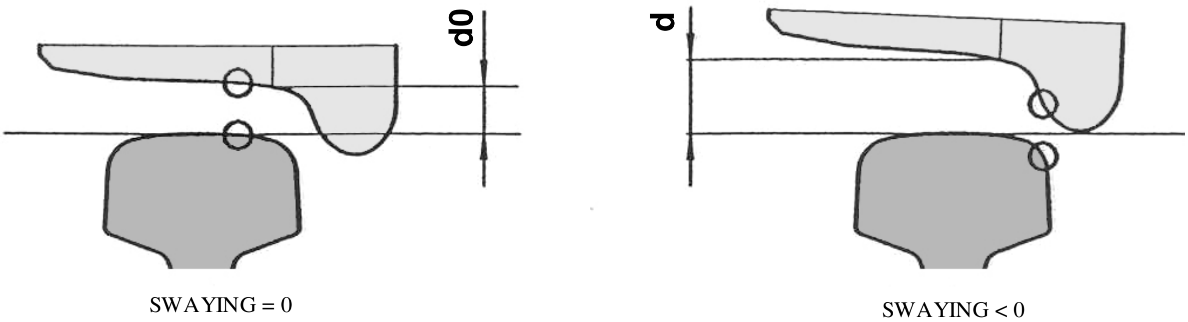

Bouncing = d – d0

Figure 14 - Definition of bouncing in computer program BCCM

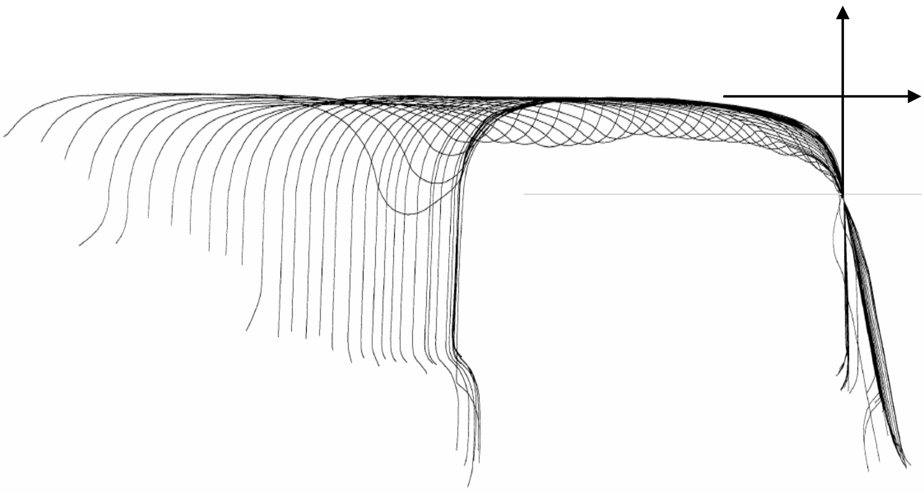

Figure 15 - Alignment of rail profiles in the switch panel

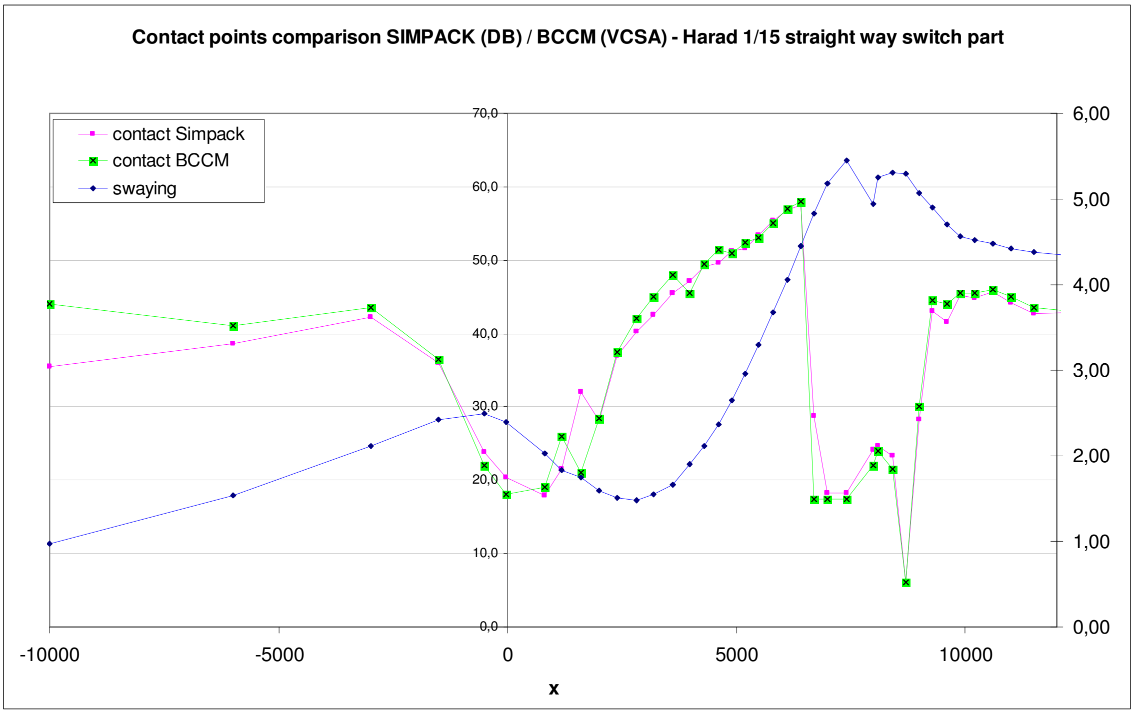

Figure 16 - Comparison of contact point locations calculated in SIMPACK and BCCM. Contact point locations are based on lateral wheelset displacement (swaying) calculated by DB. Load case: switch panel in Härad, through route, 100 km/h

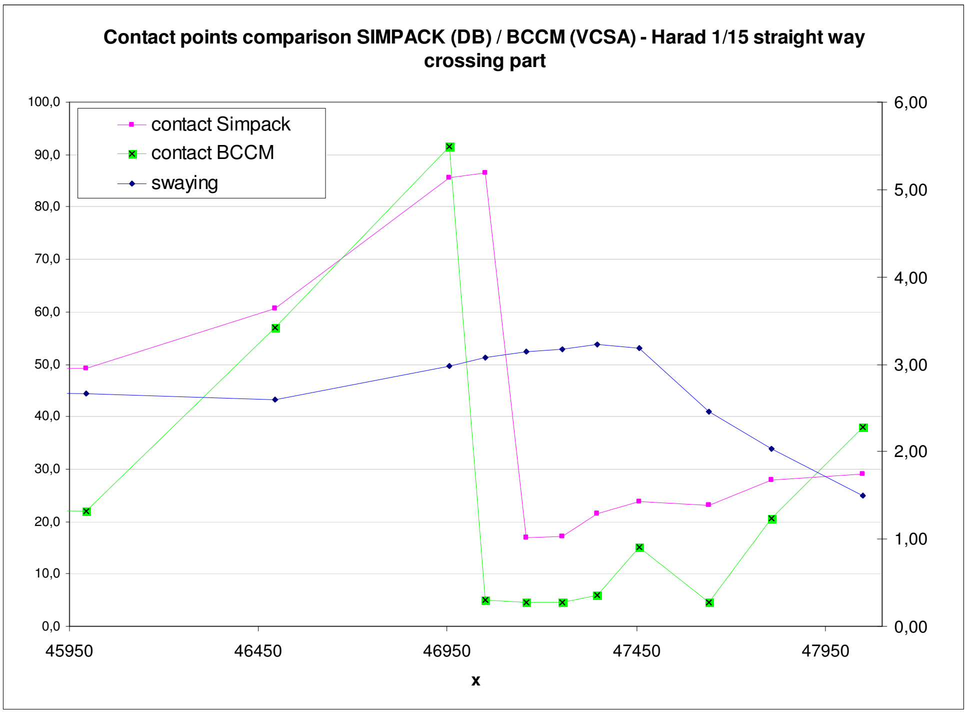

Figure 17 - Comparison of contact point locations calculated in SIMPACK and BCCM. Contact point locations are based on lateral wheelset displacement (swaying) calculated by DB. Load case: crossing panel in Härad, through route, 100 km/h

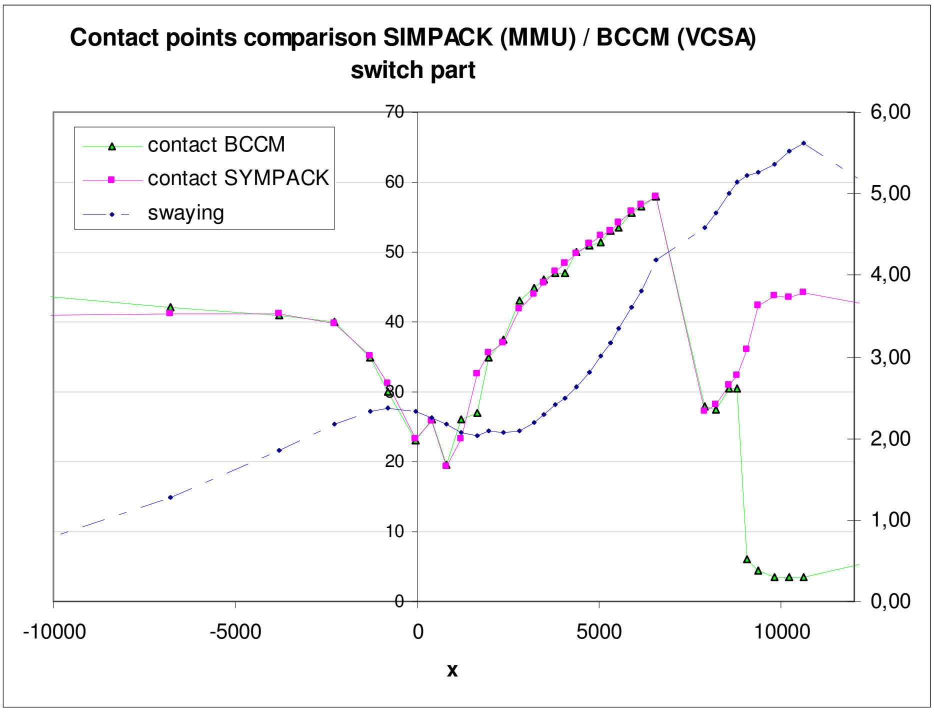

Figure 18 - Comparison of contact point locations calculated in SIMPACK and BCCM. Contact point locations are based on lateral wheelset displacement (swaying) calculated by MMU. Load case: switch panel in Härad, through route, 100 km/h

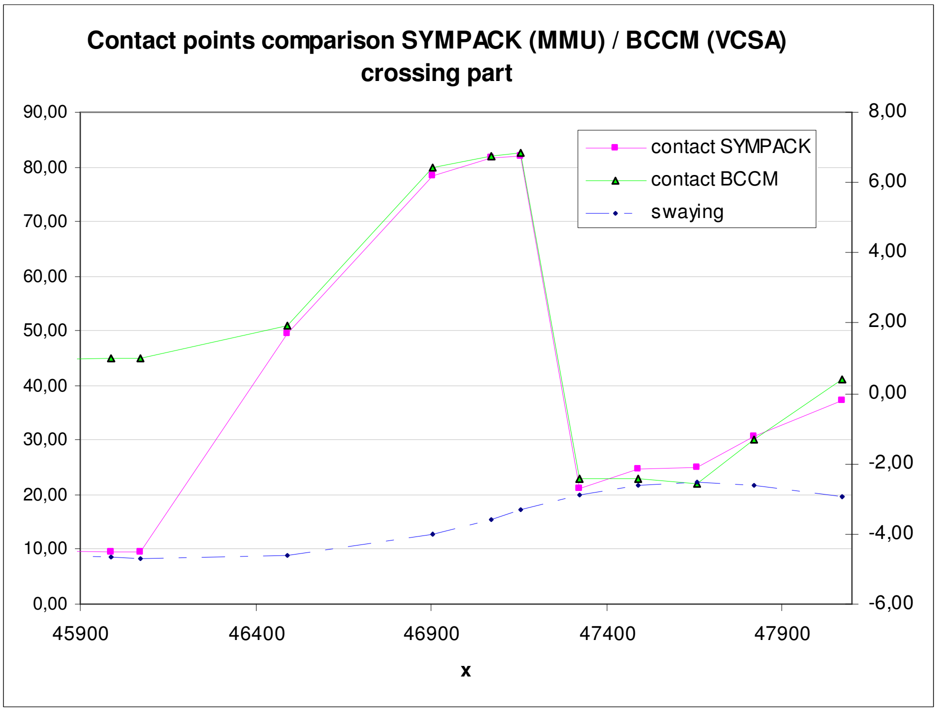

Figure 19 - Comparison of contact point locations calculated in SIMPACK and BCCM. Contact point locations are based on lateral wheelset displacement (swaying) calculated by MMU. Load case: crossing panel in Härad, through route, 100 km/h

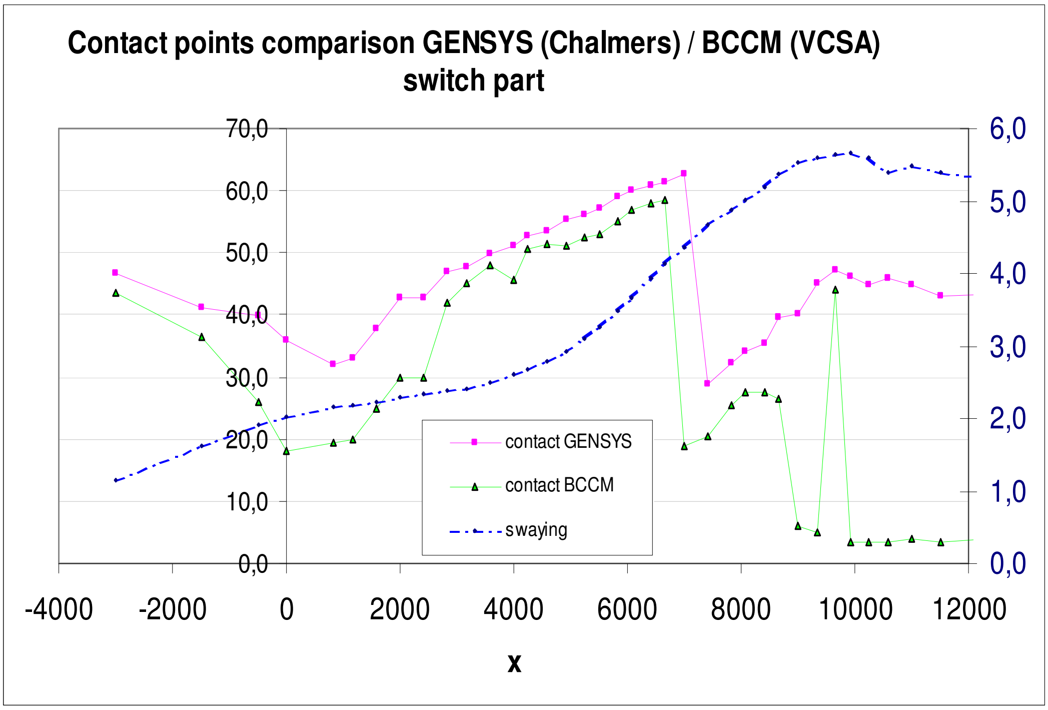

Figure 20 - Comparison of contact point locations calculated in SIMPACK and BCCM. Contact point locations are based on lateral wheelset displacement (swaying) calculated by Chalmers. Load case: switch panel in Härad, through route, 100 km/h

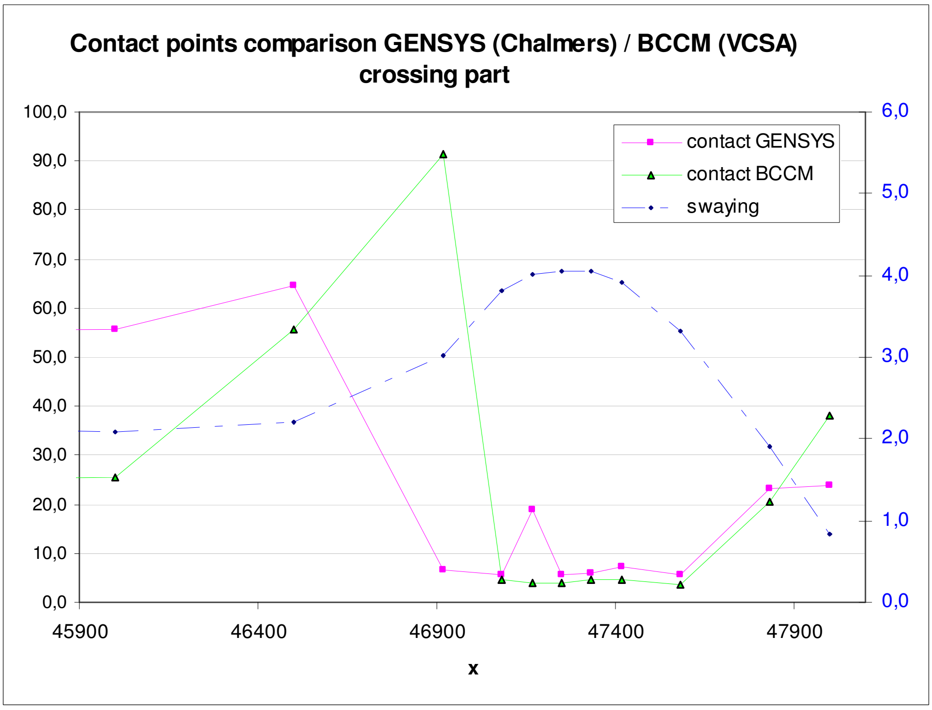

Figure 21 - Comparison of contact point locations calculated in SIMPACK and BCCM. Contact point locations are based on lateral wheelset displacement (swaying) calculated by Chalmers. Load case: crossing panel in Härad, through route, 100 km/h

5. Optimisation of dynamic track gauge – MMU

Railway vehicles often experience significant lateral displacements, sometimes leading to wheel flange contact, when running on the through route in the switch panel of railway switches. This often creates increased wheel and rail wear and in some occasions rolling contact fatigue problems on the rails, requiring increased supervision and maintenance and reducing the life of the components.

The trajectory of the wheel–rail contact on the curved stock rail and straight switch rail is illustrated in Figure 22. The transfer of the load between the stock rail and the switch rail takes place a few metres after the stock rail enters the curved path. This means that the right wheel follows the diverging route for a few metres before jumping back to the straight route. In this area, an artificial increase of the gauge is taking place on the side of the switch, and therefore a rolling radius difference is generated between the two wheels, which induces a lateral movement of the whole wheelset towards the switch rail. When the load is finally transferred to the straight switch rail a sudden reduction of the gauge takes place on one side, which causes again the wheelset to be out of the central position.

To minimise the effect of this phenomenon on the performance of the switch, a number of possible solutions have been proposed. One of the solutions is applying a dynamic variation of the gauge on the straight stock rail. Full details on the optimisation of the dynamic gauge performed by MMU are reported in Ref. [7].

This kind of system has already been commercialised by VAE under the name Fakop. However, no quantitative assessment of the achievable benefits has been found in the literature, nor a systematic design procedure to obtain optimal results in terms of reduction of wheel/rail forces and track damage.

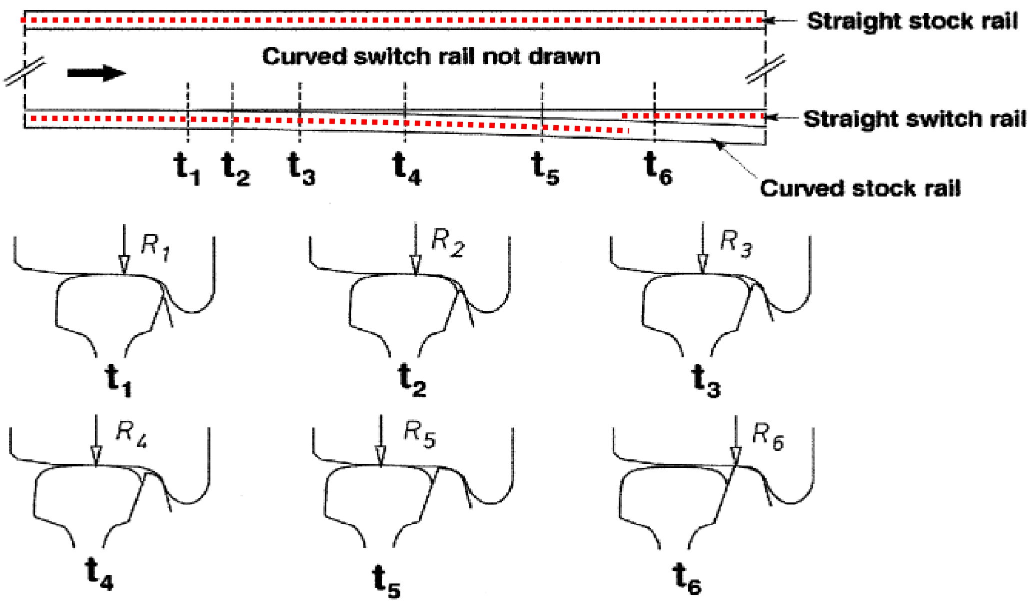

Figure 22 - Trajectory of the contact patch on the stock and switch rails. From Bugarín M R, Diaz de Villegas J M, "Improvements in railway switches", Proc. IMechEng. Part F. Journal of Rail and Rapid Transit, Vol 216, pp. 275-286 (2002)

The work by MMU aimed at answering the following questions:

- What is the optimal way of designing the dynamic gauge widening, so that wheel/rail forces and track damage can be minimised?
- What benefits can be expected in terms of reduced track damage?

In Ref. [7], a suitable design and an optimisation method based on simulation are proposed. The study started from the existing Härad switch model, see Section 4.2. The final optimised design was evaluated by simulation and the achievable benefits were quantified.

5.1 Dynamic gauge optimisation

The geometry of the gauge variation is represented in a parametric way according to Figure 23.

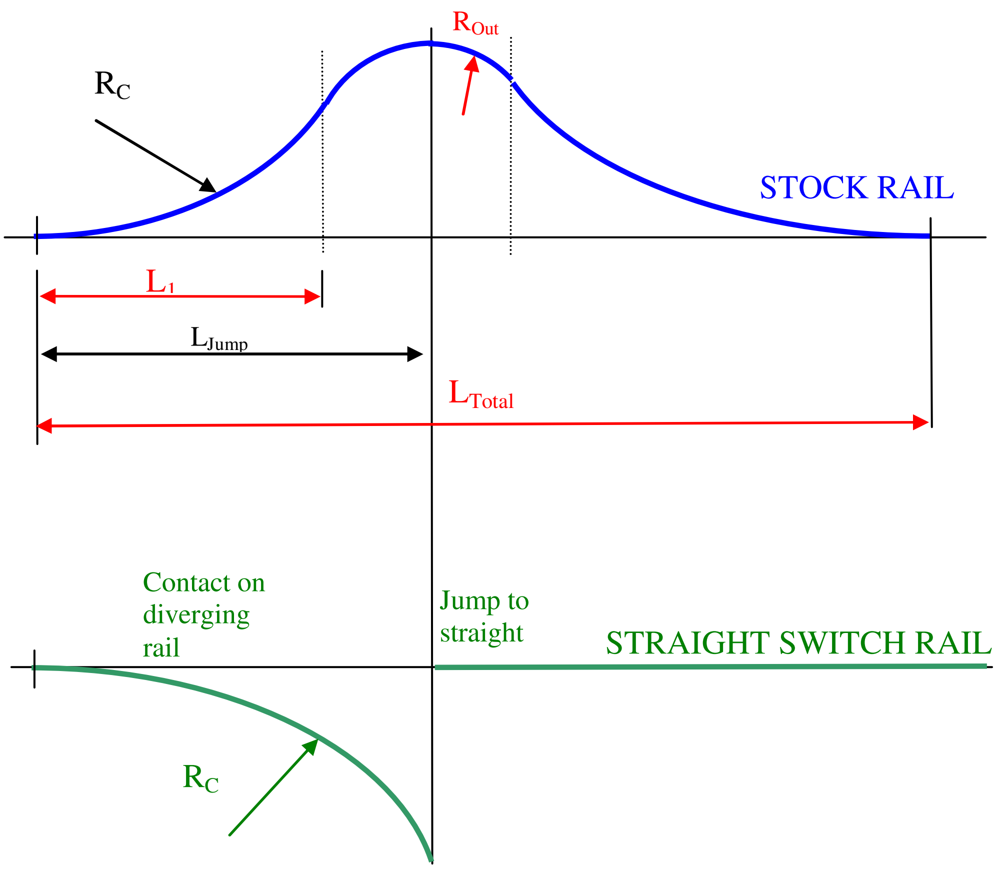

Figure 23 - Optimisation parameters for the switch rail

The dynamic gauge variation is defined by three variables or parameters:

- At the very first zone of the switch the diverging rail becomes curved with given radius R_C (corresponding to the diverging route). In this zone the same radius R_C is used for the stock rail. Thus, the track centreline is kept unchanged and the wheelset would be expected to suffer no lateral excitation. The variable L_1 represents the length for which the sign of the curvature is changed, when approaching the point where the wheel suddenly jumps to the switch rail. Assuming that the maximum amplitude of the stock rail gauge increase coincides with the point where the contact point is expected to jump from the curved rail to the switch rail, the curvature associated with this area of the dynamic gauge increase will be automatically set and will not be a variable.
- R_{OUT} is the second variable chosen for this representation model. It represents the curvature of the stock rail after the jump-point has passed.
- The third variable is L_{TOTAL} and it defines the total length of the dynamic gauge increase from the start of the switch.

These three parameters give a convenient way of defining a broad range of shapes without an excessive complexity for the subsequent optimisation process.

This process has been carried out using only one type of vehicle in the simulations. A freight vehicle with Y25 bogies is used in the laden condition, which is expected to be more harmful for the track than passenger vehicles. Also, a typical wheel profile is used. The choice of this baseline wheel profile was made on the basis of the performance observed: The vehicle was simulated running on the original switch with a total of 18 different measured wheel profiles. Then, the results in terms of traction forces, normal contact forces and contact point position on the rail were compared. With this information, a profile that showed a more or less average behaviour was chosen. The subsequent optimisation was made in terms of two outputs:

- Traction coefficient: The traction coefficient is a factor to rolling contact fatigue and, due to the influence of tangential contact forces, is at some extent related to wear.
- Contact stress: the normal stress between wheel and rail is a main factor in many aspects of rail degradation such as rolling contact fatigue and plastic deformation.

The optimisation process was carried out using this limited set of conditions. After an optimal shape for the dynamic gauge was found, a validation study was carried out using two different vehicles and more wheel profiles:

- A Y25 freight vehicle laden with 18 different measured wheel profiles
- A typical EMU, modelled using the parameters defined in SP1 of INNOTRACK, using another set of 18 measured wheel profiles.

The performance was then assessed in terms of contact energy ($T\gamma$), which represents wear, and the shakedown diagram (contact stress vs traction coefficient) which represents rolling contact fatigue.

5.2 Optimal design summary and guidelines

The optimal values chosen for the dynamic gauge increase are shown in Figure 24

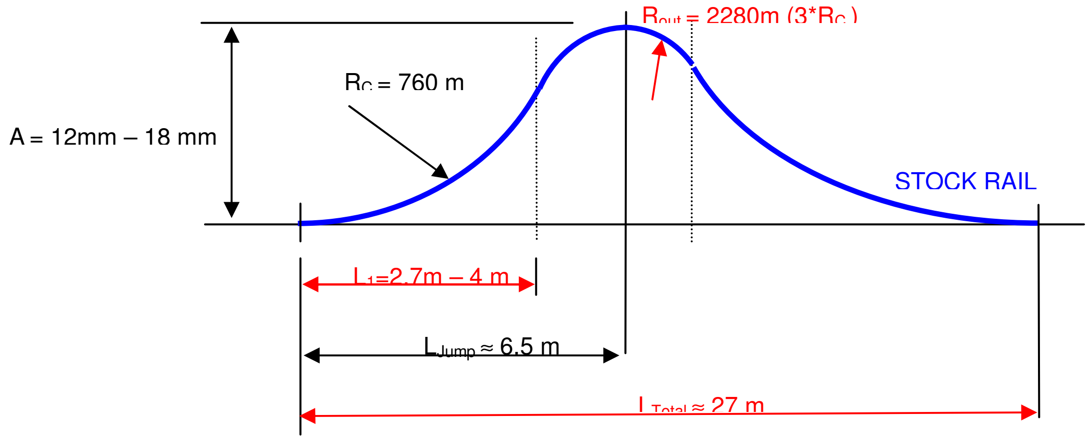

Figure 24 - Parametric representation of optimal gauge variation on the stock rail

The following guidelines could be extracted from the analysis carried out:

- The amplitude of the gauge increase (here represented by L1) is the most critical design criterion. The optimal value for this is not obvious as:
    - Tangential forces are minimised for high amplitudes of the dynamic gauge.
    - However, contact stresses show peaks, and the wheelset trajectory overruns to the opposite side.

Dynamic gauge amplitude values around half the theoretical lateral jump at the switch rail seem to give a good compromise.

- The other design parameters are less relevant to the dynamic behaviour. However, it would be recommended to have:
    - Smooth curvatures in the transition from the maximum amplitude back to the normal gauge.
    - Longer dynamic gauge increase which seems to perform a little better, but obviously care should be taken not to interfere with the crossing nose.

One example of comparison of risk for rolling contact fatigue (RCF, displayed in the form of a shakedown plot) for the different switch designs is shown in Figure 25. For each simulation, five points are plotted, one for each of five sections in which the evaluation is carried out. All the simulation cases are plotted together, but the two types of vehicle employed have been separated for clarity. The black dot markers refer to the original switch design with no gauge increase; the red square markers show the results for the optimised switch design with a maximum gauge increase of 12 mm amplitude and the green plus markers show the results for the optimised switch design with 18 mm maximum gauge increase. The limits shown in the plot are taken just as reference, as the characteristics of the materials are not known.

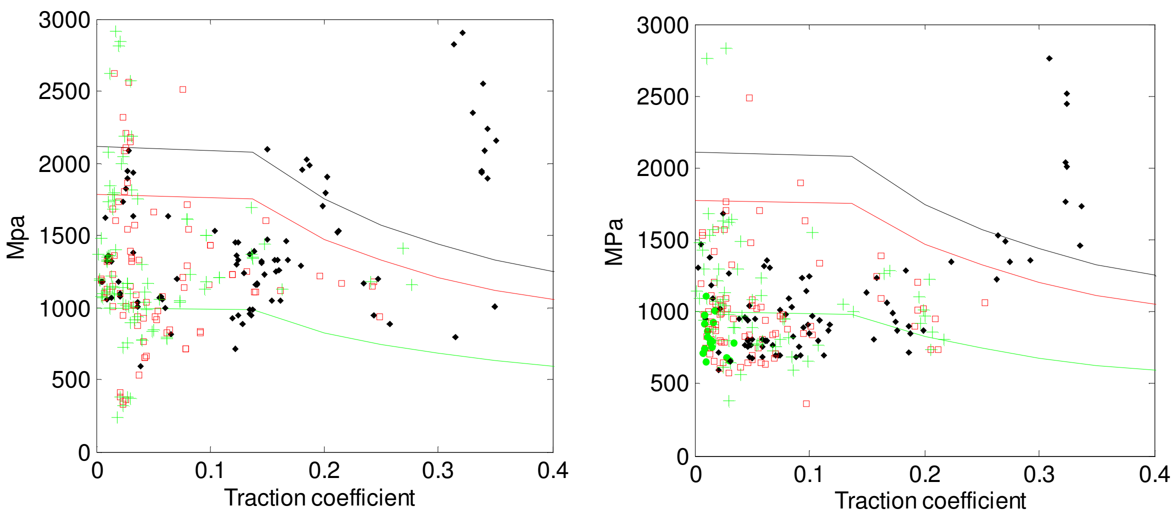

(a) Y25 freight vehicle *(b) Passenger coach*

Figure 25 - Shakedown plots for 18 wheel profiles and five rail sections

The plots show that there is a significant reduction of the risk of RCF initiation with the optimised gauge. The traction coefficients are very effectively reduced with both optimised designs. There is also a reduction in the contact stresses but this is less significant, and there are still a few values over 2000 MPa present. However, the number of these is less with the two optimised switches compared to the original one, and the traction coefficient associated with these points is also much lower.

5.3 Conclusions

The optimal design of a dynamic gauge variation has been studied and full details are provided in Ref. [7]. The use of a formal optimisation method was found too complex to be practical, given the number of possible variables, the computational load of each simulation and the number of outputs of interest. A method involving a number of simplifications has been presented and illustrated. Two possible optimal solutions were found and then these were validated by running a wider set of simulation cases on them. The main benefits obtained by the new designs proposed are:

- A very significant reduction of wear, represented by Tγ, in all locations analysed along the switch. Also, more consistency in the Tγ results when using different wheel profiles.

- A very significant reduction of the traction coefficient at all times, and therefore improved behaviour in terms of rolling contact fatigue
- Only very small or no reduction of contact stresses. In this respect, it would be advisable to carry out the dynamic gauge optimisation along with an optimisation of the shape of rail sections.

In the present optimisation, a limited number of parameters were selected to describe the geometry change. The selected parameters can define a broad range of shapes without making the optimisation process overly complex compared with applying continuously varying geometry. The amplitude of the maximum gauge widening has a big influence on the results which is related directly to one of the chosen parameters. Consistent results are obtained for different vehicle types and wheel profiles. In addition, the chosen parameters are practically achievable compared to a continuously varying geometry.

A more detailed damage analysis could provide a more accurate quantification of the benefits achievable in terms of extension of life of the components and reduction of the maintenance costs.

6. Optimisation of crossing geometry and support stiffness – DB

The objective of the work performed by DB is to optimise the crossing geometry and the supporting elasticity of the superstructure in order to minimise the contact stresses induced by wheels passing the crossing. For this purpose, the influence of different system parameters on the impact loads on a German rigid crossing EH 60-500-1:12 was studied. The simulation calculations were carried out by DB Systemtechnik with the MBS program package SIMPACK. Because of the higher speed and consequently higher impact loads compared to the diverging route, only the through route of the turnout was considered in the simulations. The full report describing the optimisation of crossing geometry and support stiffness is found in Ref. [8].

The simulations were performed with complete three-dimensional vehicle models of a Loco (BR 101) and of an ICE-T coach (BR 411) which represent different wheel loads (Loco BR 101: 107 kN, ICE-T coach: 67 kN). For the description of the wheel-rail contact geometry, three different wheel profiles were used: theoretical S1002, worn (mean) and hollow worn profile.

The track model is a finite element model (FEM) consisting of elastic rails and elastically supported elastic (concrete) sleepers which are arranged according to the layout of the turnout, (see Section 4.1 and Ref. [8]). In the cases with unsupported sleepers, the support stiffness was reduced in the transition area below one or six sleepers respectively. The reduced stiffness values were chosen so that the simulated crossing nose deflection corresponds to displacements measured on an in-service crossing with unsupported sleepers.

6.1 Proposals for modified crossing geometry

The following modified geometries of the crossing panel (crossing nose and wing rail) have been investigated by simulations, see [8]:

- Reduction of the flange way width between crossing nose and wing rail in order to shift the wheel transition area to a thicker cross-section of the crossing nose
- Modification of the nominal crossing nose profile (straight ramp) into a kinked ramp to decrease the gradient of the vertical wheel movement after transition to the crossing nose (optimisation for facing move)
- Superelevation of the wing rail and re-profiling it to better match a worn wheel profile in order to reduce the vertical wheel movement (MaKüDe)
- Modification of the wing rail profile with a chamfer to allow for hollow worn wheels to climb up the wing rail with reduced impact forces (optimization for trailing move).

The background to all these approaches is the optimisation (minimisation) of the vertical wheel movement during the transition between wing rail and crossing nose. In this way the gradient of the vertical wheel lift after the transition point can be reduced which leads to smaller impact loads on the crossing nose.

The modified wing rail design “MaKüDe” is based on the idea to provide a transition geometry which leads to a nearly horizontal wheel movement. The ramp of the crossing nose was adapted to reach a smoother transition.

The suggested wing rail profile modification was initiated by the known problem of damaged wing rails due to hollow worn wheels passing in the trailing move. In the trailing move, the outer section of the hollow worn wheel arrives to deep and hits against the profile corner of the wing rail. To avoid this, a small chamfer was added on the rail flange to reduce the contact angle when the wheel is transferred to the wing rail, see [8].

6.2 Parametric study for current crossing design

To obtain information about the distribution of the magnitude of the impact loads on crossings and to investigate the influences of operational and service parameters, a parameter study was performed. The investigated parameters were static wheel load, speed, wheel profile, lateral wheel position, maintenance state of crossing, track stiffness, unsupported sleepers and running direction.

The simulations show that impact loads in the crossing panel increase with increasing speed and wheel load, see the examples in Figure 26. The reduction of track stiffness from 500 to 85 kN/mm due to the use of elastic rail pads leads to significantly lower normal contact forces. It was concluded that a modification of track stiffness in the crossing area has a high potential for LCC reduction.

For the current crossing panel design, hollow worn wheels result in higher normal loads because of the high impact when the wheel falls down after wheel lift. A changed crossing geometry due to plastic deformation and wear leads to a notable increase of the normal loads.

The same trends in magnitudes of contact force were observed for the facing and trailing moves. However, magnitudes are higher for worn wheels in the trailing move. This is caused by the fact that the force maximum appears when the outer side of the wheel hits against the wing rail (it is common that damage appears here). Here an urgent need for action exists.

6.3 Investigation of improved designs

For the facing move with the theoretical S1002 wheel profile, the biggest contact force reduction (up to 50 kN) can be reached with the kinked ramp design whereas the MaKüDe design leads to even higher normal forces than the nominal design. For worn wheels the effect is inverted. Here the MaKüDe design provides by far the best results, see Figure 27. Considering that most wheels passing a crossing are worn, the reduced maintenance cost effect resulting from the force reduction with the MaKüDe design is anticipated to be much higher than the corresponding cost reduction with the kinked ramp design, even if there is no improvement for new wheels. Nevertheless, the MaKüDe design is subject to further development to improve also the interaction with new wheels.

For the trailing move with the theoretical S1002 wheel profile, no significant force reduction can be reached because the suggested geometry changes are targeted to the undesirable impact of worn wheels against the wing rail. For worn wheel profiles, no significant improvement is obtained except with the MaKüDe design for which the force reduction amounts to about 50 % compared to the nominal crossing design.

According to the simulation results, the conclusion can be drawn that for the most common wheel shape (represented by the mean worn wheel profile) the MaKüDe design would be the best choice as crossing geometry. Nevertheless a further optimisation based on this design could lead to a better performance also with the new S1002 profile.

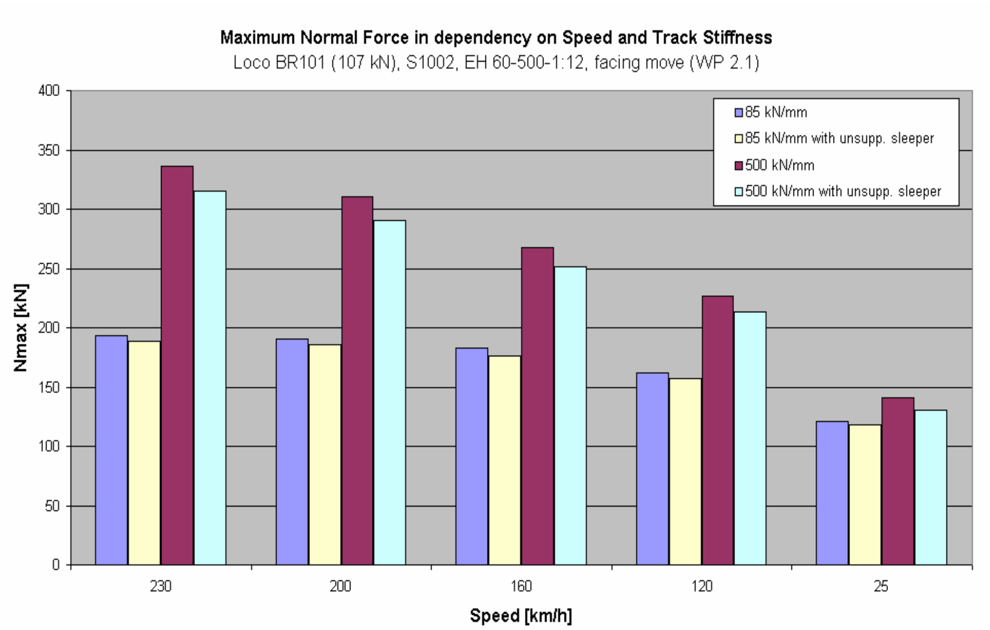

Figure 26 - Maximum normal contact force on crossing nose versus train speed and track stiffness. Loco BR 101 with S1002 wheel profiles in facing move. Nominal crossing geometry

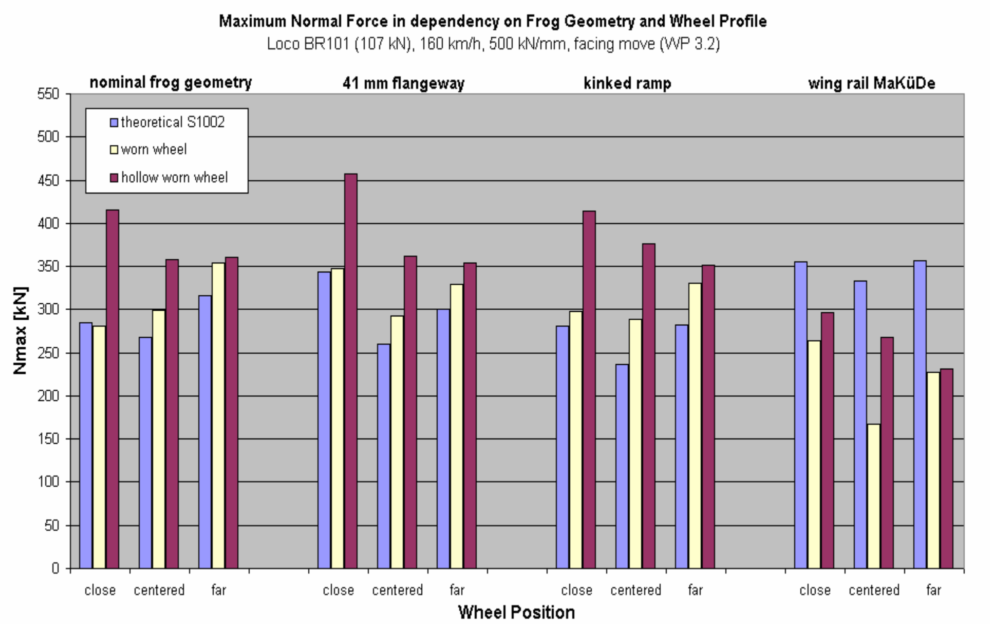

Figure 27 - Maximum normal contact force on crossing nose versus wheel position and wheel profile. Loco BR 101 in facing move. Four different crossing geometries are compared

6.4 Conclusions

By means of MBS simulations with SIMPACK, the influence of different system parameters on the impact loads on a German rigid crossing EH 60-500-1:12 was studied. The investigation was focused on the vertical track stiffness in the crossing panel, as well as on the transition geometry represented by the vertical wheel movement when passing the crossing.

The comparison of standard support stiffness with reduced stiffness values (by means of elastic rail pads) has shown that the impact loads can be reduced considerably especially for crossings passed at high speed.

Furthermore several different crossing geometries were investigated to quantify the influence of maintenance tolerances and to find an optimal design for the crossing nose and wing rails. The calculation results illustrate that it is very difficult, if not impossible, to find a solution which leads to a force reduction for all wheel profiles occurring in service. Nevertheless, the MaKüDe design developed by DB Systemtechnik showed the best performance especially for mean worn wheel profiles for both running directions (facing and trailing moves). In connection with reduced support stiffness (e.g. elastic rail pads), this crossing design will lead to a significant reduction of the impact loads and consequently a high potential for LCC reduction.

7. Optimisation of crossing geometry with BCCM – VCSA

The objective of the work performed by VCSA is to optimise the crossing geometry in order to minimise the dynamic impact induced by wheels passing the crossing. For this purpose, the resulting bouncing (vertical wheel displacement) and dip angle caused by the different crossing geometries proposed by DB (see Section 6.1 and Figure 28) on a German rigid crossing EH 60-500-1:12 were studied. The simulations were carried out by VCSA using the BCCM software.

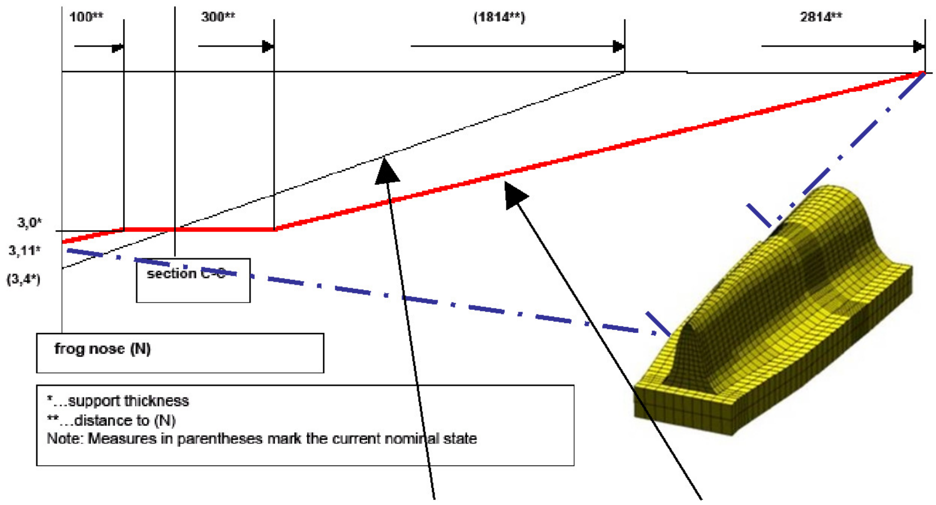

Normal frog geometry (black line) and kinked ramp (red line)

Figure 28 - Crossing geometries proposed by DB

7.1 Bouncing calculation on kinked ramp design for EH-60-500-1:12 (example)

The input to the BCCM software developed by VCSA are the cross-sections of the crossing design and the different possible wheel profiles. The wheel/crossing contact is calculated for all sections (in our example from –980/theoretical point to +1800). Examples of results calculated for the nominal crossing design or the kinked ramp design are shown in Figure 29.

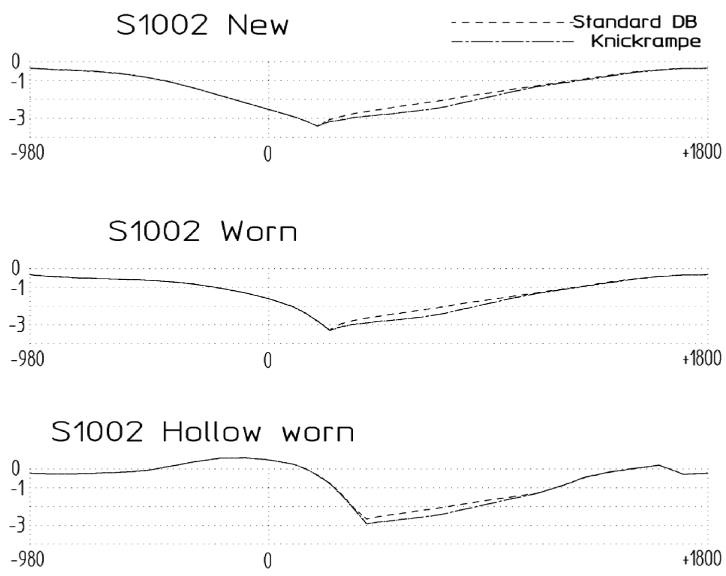

Figure 29 - BCCM (VCSA) simulation: vertical bouncing for three different wheel profiles

7.2 Bouncing results with iso-curves and dip angle for the four crossing designs

The vertical bouncing was calculated for all lateral wheel positions from –10 mm/centre of track to +10 mm/ct with a lateral spacing of 0.5 mm. See as example the bouncing curves at swaying = 0 (= centre of track). With the 3D bouncing iso-curves, a global analysis of the crossing over-running effects is obtained, see examples in Figure 30 to Figure 32.

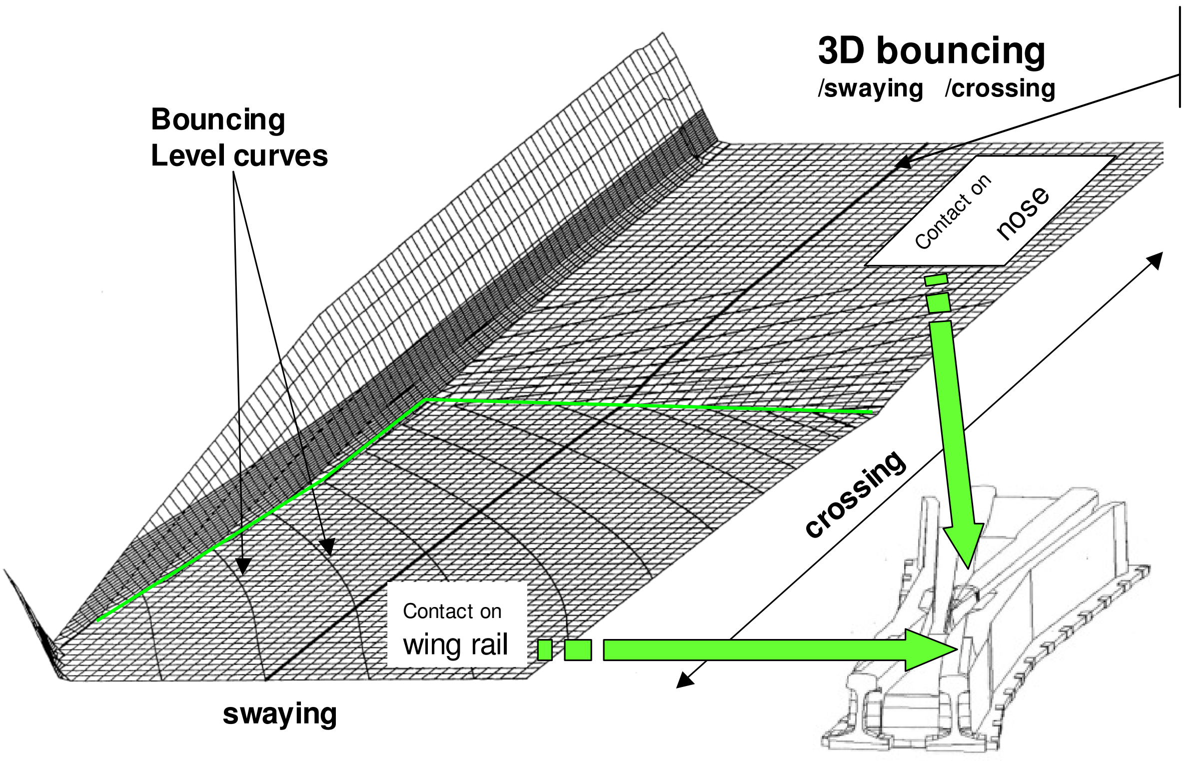

Figure 30 - BCCM bouncing level curves

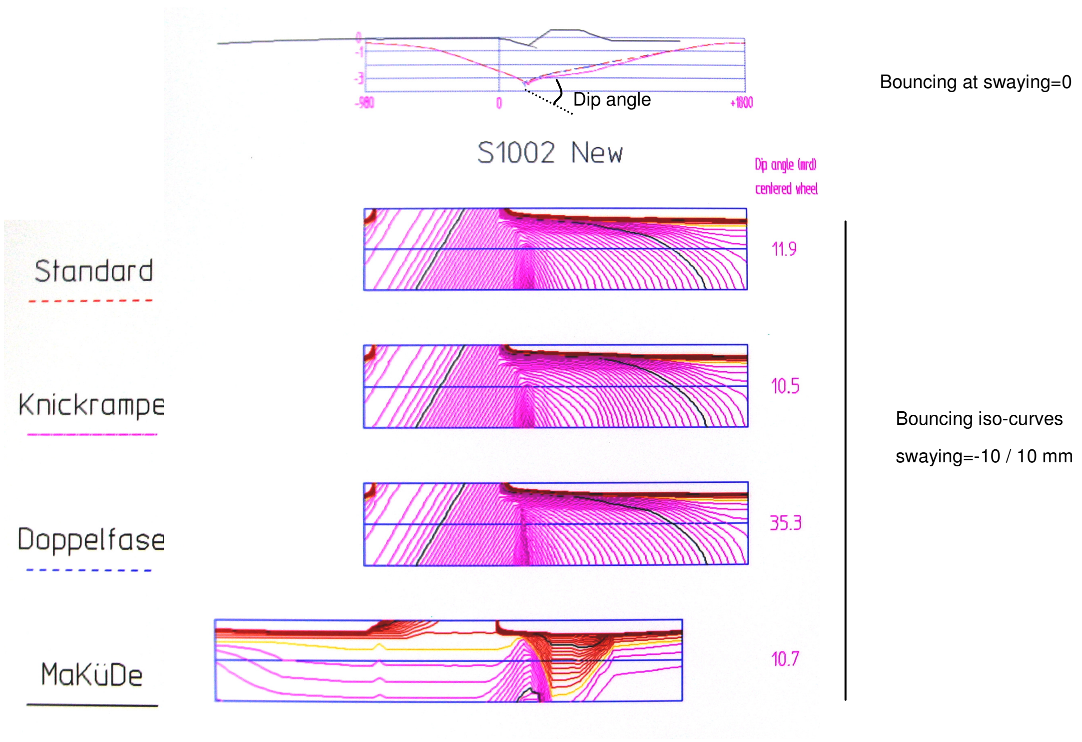

Figure 31 - Iso-curves of bouncing (vertical wheel displacement). New S1002 wheel profile on four different crossing geometries

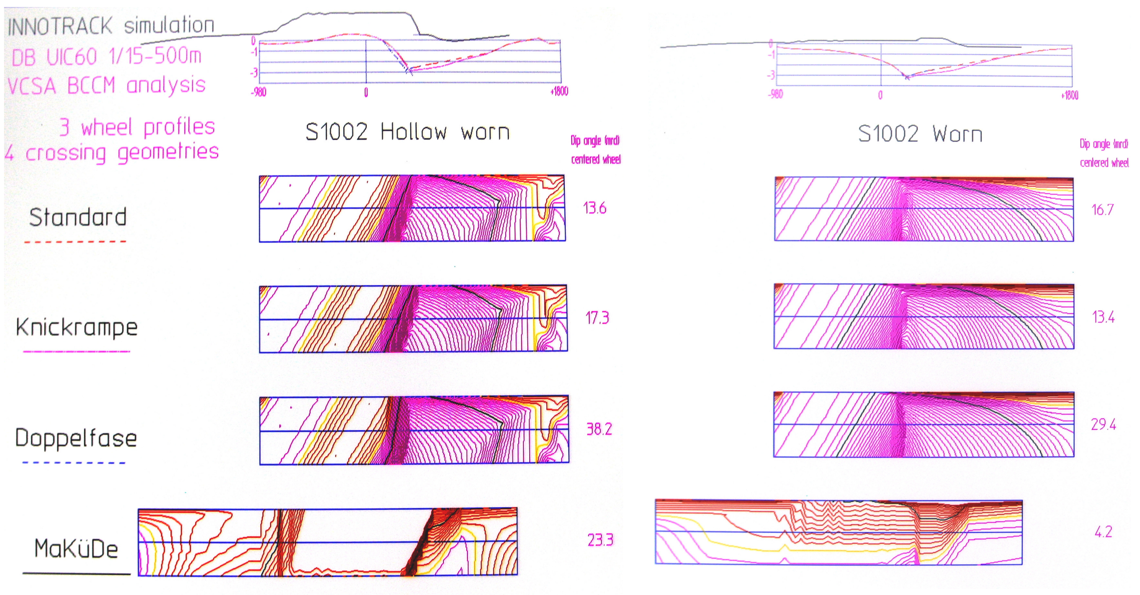

Figure 32 - Iso-curves of bouncing (vertical wheel displacement). Worn and hollow worn wheel profiles on four different crossing geometries

7.3 Conclusions

The results for the four designs (dip angle and max bouncing) are summarised in Table 1.

DB crossing TG 1/12 - R500 BCCM Wheel contact analysis

dip ang (mrd)	S1002	S1002 Worn	S1002 H.worn
Standard	11,90	16,67	13,61
Kinhed ramp	10,50	13,42	17,35
Doppelfase	35,30	29,44	38,16
MaKüDe	10,70	4,18	23,27

bouncing (mm)	S1002	S1002 Worn	S1002 H.worn
Standard	+0,6 / -2,7	-3,3	-3,4
Kinhed ramp	+0,6 / -2,9	-3,3	-3,4
Doppelfase	+0,6 / -2,9	-3,3	-3,5
MaKüDe	+2,6 / -0,13	0,55	-0,54 / +0,57

Table 1 - Calculated dip angle and maximum bouncing. Four different crossing geometries and three different wheel profiles

Based on the BCCM simulations, the investigation was focused on the vertical wheel movement when passing the crossing represented by the maximal bouncing and the dip angle as the major parameters for dynamic effects.

To find an optimal design for the crossing nose and wing rails, the bouncing and dip angle must be reduced as much as possible. The difficulty comes from the different wheel profiles which provide different effects.

For example, the MaKüDe design shows the best performance for mean worn wheel profiles but not for hollow worn wheel profiles. It is concluded that this crossing design will lead to a significant reduction of the dynamic impact loads and consequently a high potential for LCC reduction if the worn wheel profiles are limited to a non-hollow shape.

8. Conclusions

The work in INNOTRACK SP3.1 (tasks 3.1.5 Materials and 3.1.6 Optimisation) aims at the development of innovative S&C (Switches & Crossings) designs that allow for increased axle loads and lead to decreased needs for maintenance.

The present report provides an extended summary of the work performed up to December 2008. The full details on the work summarised here are given in separate reports appended to this deliverable.

A final deliverable covering the remaining work in tasks 3.1.5 and 3.1.6 is due on 2009/07/31. That report will contain results from further work on the optimisation of switch geometry and the influence of material selection on geometry degradation in the switch due to plastic deformation and wear.

9. Bibliography

[1] E Kassa and J C O Nielsen, Dynamic interaction between train and railway turnout – full-scale field test and validation of simulation models. *Vehicle System Dynamics* Vol 46, Issue S1 & 2, 2008, 521-534

[2] E Kassa and J C O Nielsen, Data from field test in turnout in Härad, INNOTRACK Technical report, June 2007, 19 pp

[3] D Nicklisch, Validation of a SIMPACK model for simulation of turnout passing, INNOTRACK Technical report, April 2008, 13 pp

[4] N Chaar and M Berg, Simulation of vehicle–track interaction with flexible wheelsets, moving track models and field tests, *Vehicle System Dynamics* Vol. 44, Supplement, 2006, 921–931

[5] E Kassa, C Andersson and J C O Nielsen, 2006, Simulation of dynamic interaction between train and railway turnout. *Vehicle System Dynamics* 44(3) 247-258

[6] T Jendel, 1997, Dynamic analysis of a freight wagon with modified Y25 bogies. M.Sc. Thesis, *Department of Vehicle Engineering, Royal Institute of Technology*, Stockholm, Sweden, 87 pp

[7] J Perez, Optimisation of the dynamic gauge for railway switches, INNOTRACK Technical report, December 2008, 25 pp

[8] D Nicklisch, SIMPACK-simulations of passing switches and crossings, INNOTRACK Technical report, December 2008, 11 pp and two appendices

10. Annexes

List of annexes

E Kassa and J C O Nielsen, Dynamic interaction between train and railway turnout – full-scale field test and validation of simulation models. *Vehicle System Dynamics* Vol 46, Issue S1 & 2, 2008, 521-534 (Appendix A in D3.1.4)

D Nicklisch, Validation of a SIMPACK model for simulation of turnout passing, INNOTRACK Technical report, April 2008, 13 pp (Appendix B in D3.1.4)

J Perez, Optimisation of the dynamic gauge for railway switches, INNOTRACK Technical report, December 2008, 25 pp (Appendix C in D3.1.4)

D Nicklisch, SIMPACK-simulations of passing switches and crossings, INNOTRACK Technical report, December 2008, 11 pp and two appendices (Appendix D in D3.1.4)